Catalysis Today 157 (2010) 303–309

Contents lists available at ScienceDirect

Catalysis Today

journal homepage: www.elsevier.com/locate/cattod

Oxidative dehydrogenation of ethane to ethylene in a membrane reactor: A theoretical study

María L. Rodriguez [a,*], Daniel E. Ardissone [b], Eleni Heracleous [c], Angeliki A. Lemonidou [c], Eduardo López [a], Marisa N. Pedernera [a], Daniel O. Borio [a]

[a] PLAPIQUI (UNS-CONICET), Camino La Carrindanga, km.7, 8000 Bahía Blanca, Argentina
[b] FICES (UNSL), Av.25 de Mayo 384, 5730 Villa Mercedes (San Luis), Argentina
[c] Chemical Process Engineering Research Institute (CERTH/CPERI), Department of Chemical Engineering, Aristotle Univ. of Thessaloniki, PO Box 1517, University Campus, GR-54006 Thessaloniki, Greece

ARTICLE INFO

Article history:
Available online 11 March 2010

Keywords:
Oxidative dehydrogenation
Ethane
Ni–Nb–O catalyst
Membrane reactor
Modeling

ABSTRACT

This contribution presents a theoretical study of a multitubular packed-bed membrane reactor for the ethane to ethylene oxidative dehydrogenation reaction over a highly active and selective Ni–Nb–O mixed oxide catalyst. This theoretical study takes into account the radial composition and temperature profiles using a two-dimensional pseudo-homogeneous model on the reaction side. The feasibility and convenience of using this novel design, as well as the influence of the main operating variables on the reactor performance, are analyzed.

The introduction of the membrane leads to lower oxygen partial pressures inside the catalyst tubes, which results in an improved selectivity to ethylene (lower heat generation rates) and high effective heat transfer area per unit volume. The multitubular membrane reactor enables significant ethylene productions per tube and milder temperature profiles than a conventional wall-cooled fixed-bed reactor. Operating conditions have to be carefully adjusted to avoid undesired oxygen accumulation inside the tubes. The presence of small amounts of oxygen at the reactor inlet significantly improves the ethylene production rates.

1. Introduction

Industrial production of ethylene is nowadays performed by thermal steam cracking (pyrolysis) of naphtha or ethane. This process is highly endothermic and requires large amounts of energy. The most promising alternative to the conventional process is the ethane oxidative dehydrogenation (ODH) to ethylene in the presence of a suitable catalyst [1,2]. In the ODH process the reactions are irreversible and exothermic; no external heating is therefore required and no equilibrium limitations are observed. The reactions proceed via a triangular series/parallel scheme with the undesired complete combustions of both ethane and ethylene. The system of reactions is represented by Eqs. (1)–(3):

$$C_2H_6 + \tfrac{1}{2}O_2 \rightarrow C_2H_4 + H_2O, \quad \Delta H_1 = -105\,\text{kJ/mol} \tag{1}$$

$$C_2H_6 + \tfrac{7}{2}O_2 \rightarrow 2CO_2 + 3H_2O, \quad \Delta H_2 = -1428\,\text{kJ/mol} \tag{2}$$

$$C_2H_4 + 3O_2 \rightarrow 2CO_2 + 2H_2O, \quad \Delta H_3 = -1323\,\text{kJ/mol} \tag{3}$$

The main disadvantage of ethane ODH is that the yield of ethylene is limited by the undesired total oxidation reactions of both ethane and produced ethylene to carbon dioxide. Deep oxidation generates a large amount of heat that can cause a runaway of the reactor and even explosions. This requires careful process control for safe plant operation. At present, ODH is not commercialized, but very intensive research activities are being carried out to develop an economically feasible process [1–3]. The research strategy is therefore twofold and based on the development of (1) highly active and selective catalysts to the desired reaction (Eq. (1)) and (2) adequate reactor technologies for an effective and safe plant operation [2].

ODH has been studied over a wide range of catalytic materials [4–12]. Many of them present the required activity; however, the majority exhibits low selectivity to the desired reaction at high conversion levels (Eq. (1)). Recently, Heracleous and Lemonidou [13,14] reported the development of bulk Ni–Nb–O mixed oxides as both highly active and selective catalytic materials for the desired reaction at low temperatures.

Multitubular reactors are commonly used in industry to carry out this type of exothermic processes, since the control of the reaction temperature is seen as a key factor to maintain adequate selectivity levels [15,16]. A previous theoretical study by our

* Corresponding author. Tel.: +54 2657 424548; fax: +54 2657 430980.
E-mail address: mlrodriguez@plapiqui.edu.ar (M.L. Rodriguez).

0920-5861/$ – see front matter © 2010 Elsevier B.V. All rights reserved.
doi:10.1016/j.cattod.2010.01.053

Nomenclature

a_i	reaction order, hydrocarbon, reaction i (dimensionless)
A_T	cross-sectional area of tubes (m^2)
b_i	reaction order, oxygen, reaction i (dimensionless)
B_0	geometric parameter of the membrane (m^2)
c_j	molar concentration of component j (kmol/m^3)
C_{pj}	specific heat of component j (kJ/(kmol K))
d_p	equivalent diameter of the catalyst pellet (momentum equation) (m)
d_T	internal tube diameter (m)
d_S	shell diameter (m)
D^e_{ij}	effective molecular diffusion coefficient of component j (m^2/s)
$D^e_{j,k}$	effective Knudsen diffusion coefficient of component j (m^2/s)
D^e_j	Bosanquet diffusion coefficient of component j (m^2/s)
D_{re}	Radial effective diffusion coefficient (m^2/s)
E_i	activation energy of reaction i (kJ/mol)
f	friction factor (dimensionless)
F_j	molar flow of component j (reaction side) (kmol/h)
F^S_j	molar flow of component j (shell side) (kmol/h)
F_T	total molar flowrate (kmol/h)
F_S	total molar flowrate, shell side (kmol/h)
J_j	permeation flow of component j (kmol/(h m^2))
k_m	membrane thermal conductivity (W/m K)
$k_{R,i}$	pre-exponential constant, reaction i (kmol/(s kg_{cat} $Pa^{(ai+bi)}$))
K_0	geometric parameter of the membrane (m)
M_j	molecular weight of component j (kg/kmol)
n_T	number of tubes
NC	number of components
NCP	number of components permeated through the membrane
NR	number of reactions
L	tube length (m)
p_j	partial pressure of component j (tube side) (Pa)
P	total pressure (reaction side) (Pa)
P_S	total pressure (shell side) (Pa)
P_m	average pressure (Pa)
r	radial coordinate (m)
r_i	reaction rate, reaction i ($kmol_{CH}$/(kg_{cat} s)) where HC=C_2H_6 (reactions (1) and (2)) and HC=C_2H_4 (reaction (3))
R	universal gas constant (kg m^2/(kmol s^2 K))
S_G	global selectivity (dimensionless)
S_I	instantaneous selectivity (dimensionless)
T	temperature (reaction side) (K)
T_m	average temperature (K)
T_R	reference temperature (K)
T_S	temperature (shell side) (K)
U	overall heat transfer coefficient (kJ/(h m^2 K))
u_S	superficial velocity (m^3_f/(m^2_r s))
y_j	molar fraction (mol_j/mol_{total})
z	axial coordinate (m)

Greek Letters

α	heat transfer coefficient (kJ/(h m^2 K))
δ	membrane thickness (m)
ΔH_{ri}	heat of reaction of reaction i (kJ/mol)
$\Delta P_{T\text{-}M}$	pressure drop across the membrane (atm)
$\Delta\rho_g$	difference between gas density values corresponding to two adjacent axial positions (kg/m^3_f)
Δz	difference between two adjacent axial positions (m)
λ_{re}	radial effective conductivity (kJ/(h m K))
ρ_g	gas density (kg/m^3_f)
ρ_B	bed density (kg_{cat}/m^3)
μ_j	viscosity of component j (Pa s)

Subscripts and superscripts

i	reaction i
j	component j
k	component k
0	at the axial coordinate $z = 0$
L	at the axial coordinate $z = L$
S	shell side
T	tube side
C_2H_6	ethane
C_2H_4	ethylene
CO_2	carbon dioxide
H_2O	water
O_2	oxygen

investigation group [16] of a multitubular fixed-bed reactor for the ODH of ethane over the Ni–Nb–O catalyst demonstrated that such reactor configuration is feasible, provided that high heat transfer area per unit volume and low oxygen concentrations along the tube are maintained. A two-bed multitubular reactor with intermediate air injection proved to be superior to a single-bed design, yielding higher ethylene production rates due to increased ethylene selectivity.

An attractive alternative to these fixed-bed reactors is the use of a membrane reactor to axially distribute the oxygen in the reaction medium (see Fig. 1). As reported by Heracleous and Lemonidou [13,14], lower oxygen partial pressures increase the ethylene selectivity and yield and decrease the generated heat.

The advantages of the application of membrane reactors on oxidative dehydrogenation have been largely demonstrated at laboratory scale for ethane [17–19], propane [20,21] and butane [22,23]. The interest and progress in this field within the last two decades is very well reflected in extensive literature reviews that have been published in recent years [24–30]. It is common consensus in literature that the use of membrane reactors in selective oxidation reactions outperforms the conventional fixed-bed reactors in both olefin yield and selectivity at low feed ratios. The oxygen distribution also allows better heat management, which leads to lower local reaction rates and, consequently, lower rates of heat generation [17,18,31]. Furthermore, in the case of flammable mixtures, as in this case, the oxygen distribution through the membrane prevents the local generation of dangerous concentrations and allows an operation under normally prohibitive reaction mixture concentrations, reducing the formation of hot spots and flames [18,26,31,32].

An inorganic porous membrane is proposed in the present work to axially distribute the required oxygen. The inert membrane tubes are assumed to be filled with catalyst particles, and oxygen is dosed from the shell side through the membrane into the tubes, as shown in Fig. 1. This inorganic membrane allows higher

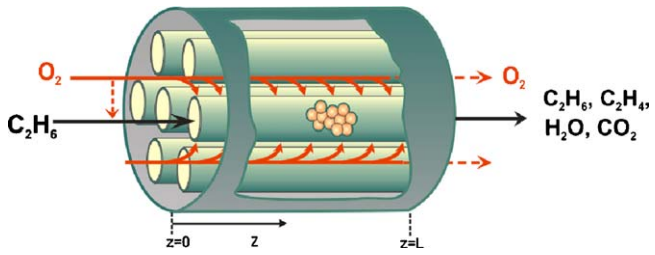

Fig. 1. Scheme of the ethane ODH membrane reactor.

permeation fluxes than those of dense membranes [17,23,31], which is desirable to favor the reaction ignition. The use of dense oxide membranes to feed O_2 to partial oxidation reactions is limited by the need of high temperatures to obtain reasonable permeation rates [27,28,33]. Moreover, dense membranes show limited thermal and chemical stability upon aging [18,26,27,33]. Several modeling studies of membrane reactors with oxygen distribution for oxidative dehydrogenation [22,31,34–37] including our previous theoretical study for oxidative dehydrogenation of ethane [38] have reported the advantages of this reactor configuration.

Most of these studies consider that the radial concentration and temperature profiles are flat. This approach is probably correct for most laboratory-scale reactors, where the diameters of the bed are small (only a few millimeters); however, in the case of a commercial-scale reactor, it is necessary to consider the effects of mass and heat transfer in the radial direction. The use of a 2D model is expected to result in more precise estimations of the performance of large-scale membrane reactors.

In this work, the theoretical study of ethane ODH over a Ni–Nb–O mixed oxide catalyst is further investigated by analyzing the feasibility and convenience of using a novel membrane reactor design by means of a 2D pseudo-homogeneous model. To our knowledge, this is the first time that the use of a 2D model of a membrane reactor for ODH of ethane is reported. The influence of the main operating variables on the reactor performance is also addressed.

2. Mathematical model

A two-dimensional, pseudo-homogeneous, steady-state model has been used to represent ethane ODH in a multitubular packed-bed membrane reactor. Considering the use of high total flowrates through the packed-bed, axial mass and energy dispersions and external transport limitations were assumed to be negligible. Internal mass- and energy-transport limitations were also neglected because a thin washcoat over the catalyst particles (egg-shell type) was chosen [16,38].

The reactor shell was assumed to be properly isolated with negligible heat losses to the environment. Ergun's friction factor was employed to predict the pressure drop inside the tubes [39], while isobaric conditions were selected for the O_2 flowing on the shell side.

The catalyst particles were assumed to be hollow cylinders (Raschig-ring type) of 6 mm × 6 mm × 2 mm in order to diminish the pressure drop along the reactor length. A bed void fraction of 0.48 was considered in the simulations, in agreement with literature [40]. The washcoat covering the hollow cylinders, where the active components were impregnated, was assumed to have a mean thickness of 177 μm. The use of washcoated particles resulted in a low bed density of $\rho_B = 200\ kg_{cat}/m^3$, which favored the moderation of the heat generation rate per unit volume and, consequently, achieved milder operating conditions.

Table 1
Geometrical parameters and operating conditions.

L	4 m
d_T	2.66 cm
d_S	3.93 m
n_T	12000
P_0	5 atm
P_S	5.15–5.45 atm
$F_{0,T}$	4400 kmol/h
Catalyst type	Hollow cylinders
d_p	0.0045 m
ρ_B	200 kg/m^3
$F_{0,S}$	3000 kmol/h
T_0	370 °C, 400 °C, 430 °C
T_{S0}	25 °C
y_{0,O_2}	0–0.01
y_{0,C_2H_6}	0.99-1

The overall heat transfer coefficient (U) was evaluated as resistances in series on the tube and shell sides. The corresponding heat transfer coefficients (α_T and α_S) were calculated from the data fitted by Yagi and Kunii [41] and the Delaware method [42], respectively. The global selectivity (S_G) was calculated as the ratio between the amount of ethylene produced and the amount of ethane consumed, from the reactor inlet to the desired axial coordinate.

To avoid the multiplicity of steady states inherent in counter-current operation, a cocurrent flow configuration between the process gas and the oxygen in the shell was selected. The cocurrent scheme also lowers the hot spots, which leads to longer catalyst life and reduces the parametric sensitivity, which ensures safe operating conditions [43]. The reactor was assumed to be cooled both by convective heat exchange between reactants and coolant and by cold-shot of oxygen permeated through the membrane.

The radial effective diffusion coefficient (D_{re}) was adopted from Froment and Bischoff [39], and the radial effective conductivity (λ_{re}) was calculated following the guidelines suggested by Zehner and Schlünder [44]. The geometrical parameters of the reactor and catalyst as well as the main operating conditions are reported in Table 1. Table 2 compiles geometrical parameters [45] and thermal conductivity [46] of the inert ceramic membrane selected here.

Reaction side (catalyst tubes):

Total mass balance

$$\frac{\partial(u_s\rho)}{\partial z} = \frac{4}{d_T} J_{O_2} M_{O_2} \tag{4}$$

Component mass balances

$$\frac{\partial(u_s c_j)}{\partial z} = D_{re}\left(\frac{\partial^2 c_j}{\partial r^2} + \frac{1}{r}\frac{\partial c_j}{\partial r}\right) + r_j \tag{5}$$

with $j = C_2H_6\,(1), C_2H_4\,(2), O_2\,(3), H_2O\,(4), CO_2\,(5)$

where the permeation flux is quantified by the following expression [47]:

$$J_j = -\frac{1}{RT_m}\left[\frac{D_j^e}{\delta}(p_j - p_{j,S}) + \frac{B_0}{\delta\mu_j} p_{j,S}(P - P_S)\right] \quad j = O_2 \tag{6}$$

$$D_j^e = \left(\frac{1}{D_{ij}^e} + \frac{1}{D_{j,k}^e}\right)^{-1} \tag{7}$$

Table 2
Parameters of the membrane [19,20].

K_0 (×10^{10} m)	23.1
B_0 (×10^{17} m^2)	11.5
δ (m)	0.00175
k (W/m K) (at T = 300 °C)	16.06

$$D^{e}_{j,k} = K_0 \sqrt{\frac{8RT}{\pi M_j}} \tag{8}$$

Energy balance

$$\frac{\partial T}{\partial z} = \frac{1}{u_S} \frac{1}{\sum_{j=1}^{NC} c_j C_{pj}} \left[\sum_{i=1}^{NR} r_i(-\Delta H_i) + \lambda_{re} \left(\frac{\partial^2 T}{\partial r^2} + \frac{1}{r} \frac{\partial T}{\partial r} \right) \right] \tag{9}$$

Momentum equation

$$\frac{dP}{dz} = -\frac{f \rho_g u_S^2}{d_p} \tag{10}$$

Shell side:

Mass balance

$$\frac{dF_j^S}{dz} = -J_j \pi d_T n_T, \quad j = O_2\ (3) \tag{11}$$

Energy balance

$$\frac{dT_S}{dz} = \frac{U \pi d_T n_T (T - T_S)}{F_j C_{pj}}, \quad j = O_2\ (3) \tag{12}$$

Boundary conditions

- At $z = 0$, $\forall\ r$ (inlet condition):

$$c_j = c_{j0}, \qquad T = T_0, \qquad P = P_0, \qquad T_S = T_{0S}, \qquad P_S = P_{0S} \tag{13}$$

- At $r = 0$, $\forall\ z$ (symmetry condition):

$$\frac{\partial c_j}{\partial z} = 0, \qquad \text{for } j = C_2H_6\ (1), C_2H_4(2), O_2\ (3), H_2O\ (4), CO_2\ (5) \tag{14}$$

$$\frac{\partial T}{\partial z} = 0 \tag{15}$$

- At $r = R$, $\forall\ z$ (membrane wall condition):

$$\frac{\partial c_j}{\partial z} = 0 \quad \text{for } j = C_2H_6\ (1), C_2H_4\ (2), H_2O\ (4), CO_2\ (5) \tag{16}$$

$$\frac{\partial c_j}{\partial z} = \frac{J_j}{D_{re}} \quad \text{for } j = O_2\ (3) \tag{17}$$

$$\frac{\partial T}{\partial r} = \frac{(U + J_{O_2} C_{p_{O_2}})}{\lambda_{re}} (T_S - T) \tag{18}$$

Kinetic model equation:

The power-law kinetic model proposed by Heracleous and Lemonidou [14] for reactions (1)–(3) over a $Ni_{0.85}Nb_{0.15}O$ catalyst was used for the simulations:

$$r_i = k_{R,i} \exp\left[-\frac{E_i}{R} \left(\frac{1}{T} - \frac{1}{T_R} \right) \right] p_{HC_i}^{a_i} p_{O_2}^{b_i} \tag{19}$$

3. Results and discussion

3.1. Influence of the inlet temperature on the tube side (T_0)

Fig. 2 shows the axial temperature profiles on the tube and shell sides, for three different feed temperatures. The solid curves represent the radial mean temperature on the tube side, along the reactor length. The inlet temperature on the shell side is kept constant at 25 °C. A small amount of O_2 is fed at the reactor inlet ($y_{0,O_2} = 0.01$) and the main O_2 feed is permeated through the membrane. A constant trans-membrane pressure drop of 0.45 atm is selected. At the lowest feed temperature (T_0 = 370 °C), the heat transfer rate to the shell side is higher than the heat generation rate

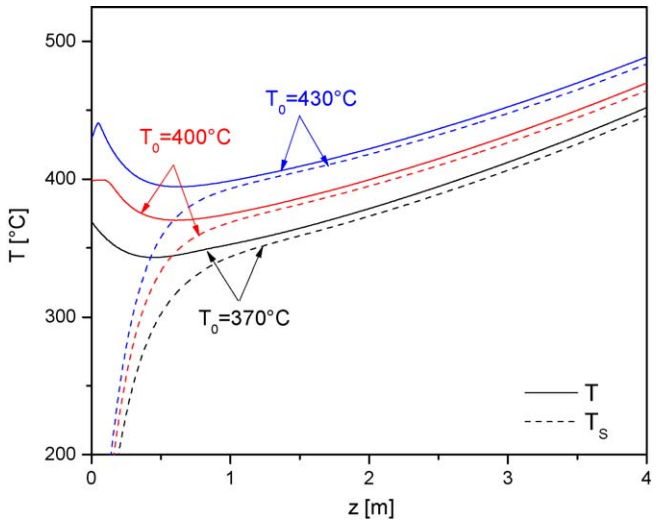

Fig. 2. Axial temperature profiles for T_0 = 370, 400 and 430 °C. Solid lines: radial mean temperature of the reaction side. Dashed lines: shell side temperature. $T_{0,S}$ = 25 °C; $y_{0,O_2} = 0.01$; $\Delta P_{T\text{-}M}$ = 0.45 atm.

and so the process stream is initially overcooled. After reaching a minimum, the temperature shows a continuous and smooth increase up to the reactor outlet. Beyond 1.5 m, the temperature profiles on both reactor sides (T and T_S) practically overlap. The behavior for T_0 = 400 °C is similar and the average thermal level of the reactor is around 25 °C over that of T_0 = 370 °C. For the highest feed temperature (T_0 = 430 °C), the reactor temperature is still under control, though a small hot spot appears near the reactor inlet. This maximum is associated both with the high feed temperature and the initial oxygen content (1%), which lead to high heat generation rates.

Fig. 3 shows the radial mean O_2 molar fraction for the same conditions as Fig. 2. As shown, the O_2 content inside the catalyst tubes drops from its initial value ($y_{0,O_2} = 0.01$) to nearly zero. This sharp drop in the O_2 concentration is more pronounced at higher inlet temperatures due to the higher reaction rates. Once the oxygen content reaches low enough values, the O_2 permeation rate through the membrane tubes is nearly balanced with the O_2 consumption rate by chemical reaction. Consequently, the ethylene production rate is controlled by the O_2 permeation rate. This phenomenon can be seen in Fig. 3, where an almost linear increase of the ethylene productivity per tube is observed for $z > 1.5$ m. The similar ethylene production rates for the three T_0 values reveals that the O_2 permeation rate is not strongly affected by temperature. The low O_2 concentrations along the tube enable high outlet selectivity to ethylene (95–97%) as the reaction order of the desired reaction (Eq. (1)) is lower than those of the combustion reactions (Eqs. (2) and (3)) [10]. This outstanding selectivity level also helps to control the reactor temperature (Fig. 2), due to the reduced extents of the highly exothermic combustion reactions.

3.2. Influence of the oxygen feed content (y_{0,O_2})

Two different oxygen feed distributions are compared in this section. Fig. 4 shows the temperature evolution inside the reactor for $y_{0,O_2} = 0$ (no oxygen in the reactor inlet) and $y_{0,O_2} = 0.01$ (feed composition: 99% C_2H_6, 1% O_2). The temperature profiles are similar for both feeds, showing a minimum in the first tube zone followed by a smooth increase. The temperature level for the case $y_{0,O_2} = 0.01$ is around 30 °C higher than that for $y_{0,O_2} = 0$ due to the higher total amount of heat being generated by the exothermic reactions. The additional amount of O_2 fed to the reactor mouth contributes to increased ethylene production

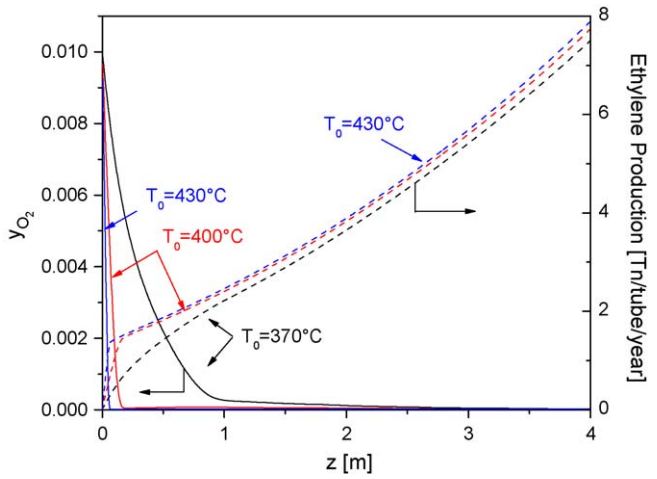

Fig. 3. Oxygen molar fraction along the reactor length (radial mean values), for the conditions of Fig. 2. Right ordinate axis: ethylene flowrate per tube.

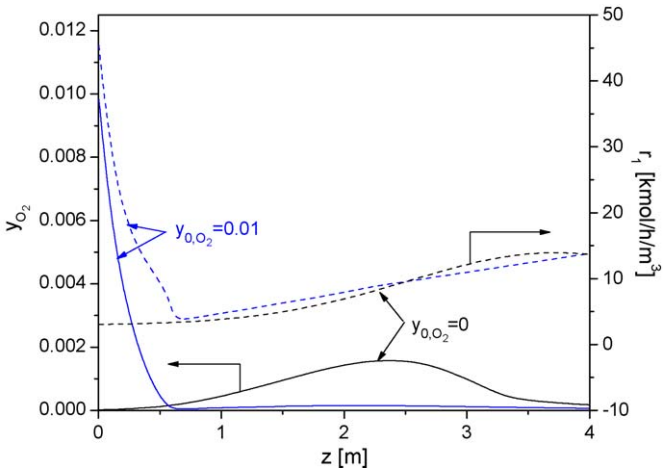

Fig. 5. Oxygen molar fraction along the reactor length (radial mean values), for the conditions of Fig. 4. Right ordinate axis: rate of reaction 1 (ethane ODH, see Eq. (1)).

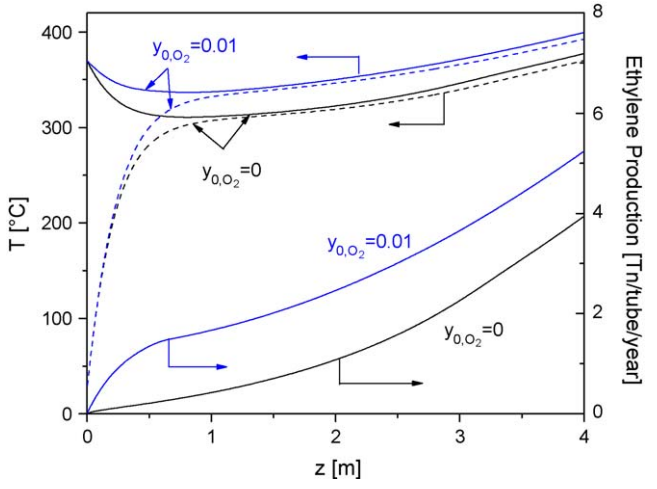

Fig. 4. Axial temperature profiles for $y_{0,O_2} = 0$ and 0.01. Solid lines: radial mean temperature of the reaction side. Dashed lines: shell side temperature. Right ordinate axis: ethylene flowrate per tube. T_0 = 370 °C; $T_{0,S}$ = 25 °C; $\Delta P_{T\text{-}M}$ = 0.15 atm.

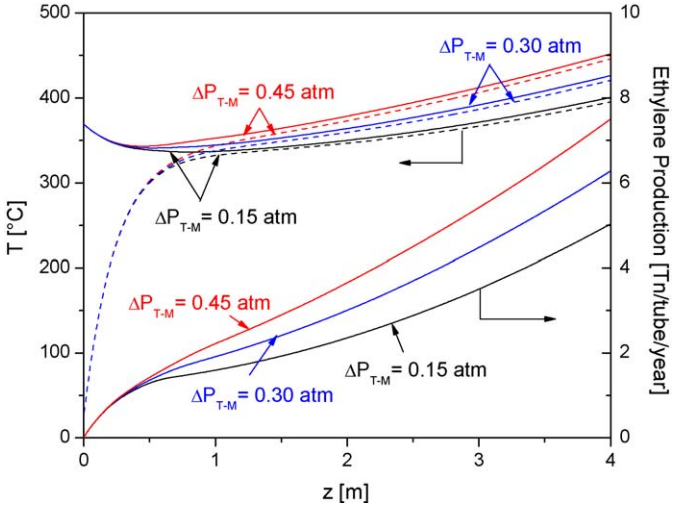

Fig. 6. Axial temperature profiles for $\Delta P_{T\text{-}M}$ = 0.15, 0.30 and 0.45 atm. Solid lines: radial mean temperature (reaction side). Dashed lines: shell side temperature. Right ordinate axis: ethylene flowrates per tube. T_0 = 370 °C; $T_{0,S}$ = 25 °C; y_{0,O_2} = 0.01.

in the first 0.5 m of the reactor, with respect to the case of $y_{0,O_2} = 0$ (Fig. 4). Downstream z = 1 m, the curves of ethylene flowrates are practically parallel, which indicates that the instantaneous ethylene production rates are similar for both feed conditions. The corresponding radially averaged oxygen profiles inside the catalyst tubes are shown in Fig. 5. In the case of $y_{0,O_2} = 0.01$, the reaction rates are high enough to cause a fast oxygen consumption close to the reactor inlet. When no oxygen is fed at z = 0, the reaction rates are lower and O_2 is accumulated. Under these operating conditions, the permeation rate though the membrane exceeds the oxygen consumption rate. The gradual increase in the partial pressure of O_2 leads to higher reaction rates and the oxygen content inside the tube decreases again, close to the reactor outlet. This accumulation phenomenon is clearly undesired, since it can lead to selectivity losses and safety problems associated to the possible occurrence of explosive mixtures.

3.3. Influence of the oxygen permeation flux

The permeation flux through the membrane is varied by applying different trans-membrane pressure drops ($\Delta P_{T\text{-}M}$). This was done by adjusting the pressure on the shell side to satisfy the desired $\Delta P_{T\text{-}M}$ value. Fig. 6 shows the influence of the parameter $\Delta P_{T\text{-}M}$ on the axial profiles of temperatures (T and T_S) and the ethylene flowrate per tube. The temperature can be seen to increase with the amount of permeated oxygen. Nevertheless, even for $\Delta P_{T\text{-}M}$ = 0.45, the temperature level keeps within tolerable limits. It is important to note that the production rate is determined by the permeated oxygen. In fact, the outlet production rate increases around 50% when the trans-membrane pressure drop is increased from 0.15 to 0.45 atm. It is worth mentioning that the outlet global selectivity does not deteriorate for this threefold variation in $\Delta P_{T\text{-}M}$ as no oxygen accumulation occurs ($0.955 < S_G < 0.962$).

Radial profiles of oxygen molar fraction are presented in Fig. 7 for different axial positions, for the case $\Delta P_{T\text{-}M}$ = 0.45. The corresponding radial temperature profiles are reported in Fig. 8. Two types of oxygen profiles can be seen. For axial positions close to the reactor inlet ($z < 0.5$ m), nearly flat profiles are calculated as the oxygen fed at the reactor mouth is not completely consumed. This behavior is associated to radial temperature profiles which are typical of wall-cooled fixed-bed reactors, i.e., the temperature decreases towards the tube wall. For axial coordinates $z > 1$ m,

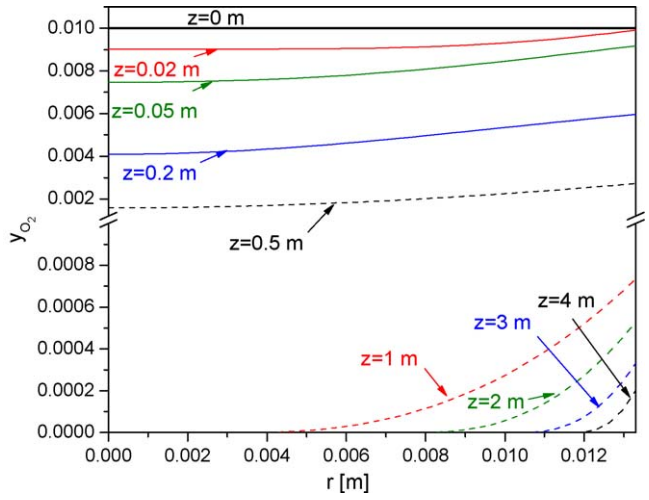

Fig. 7. Radial profiles of oxygen molar fraction, for different axial positions. T_0 = 370 °C; $T_{0,S}$ = 25 °C; $y_{0,O_2} = 0.01$; $\Delta P_{T\text{-}M}$ = 0.45 atm.

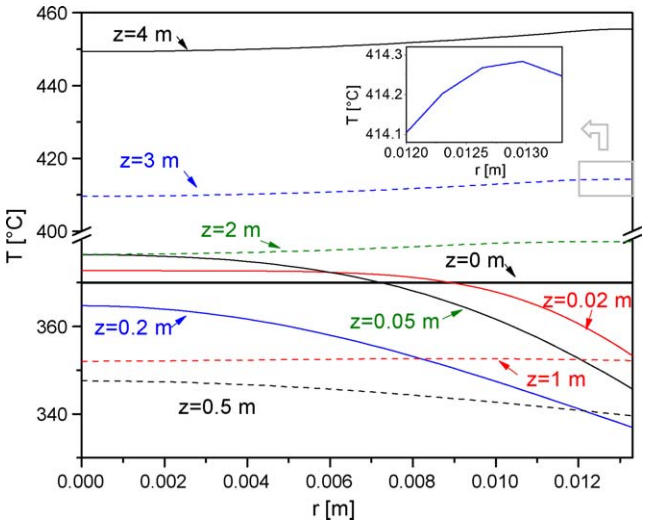

Fig. 8. Radial temperature profiles for different axial positions. T_0 = 370 °C; $T_{0,S}$ = 25 °C; $y_{0,O_2} = 0.01$; $\Delta P_{T\text{-}M}$ = 0.45 atm.

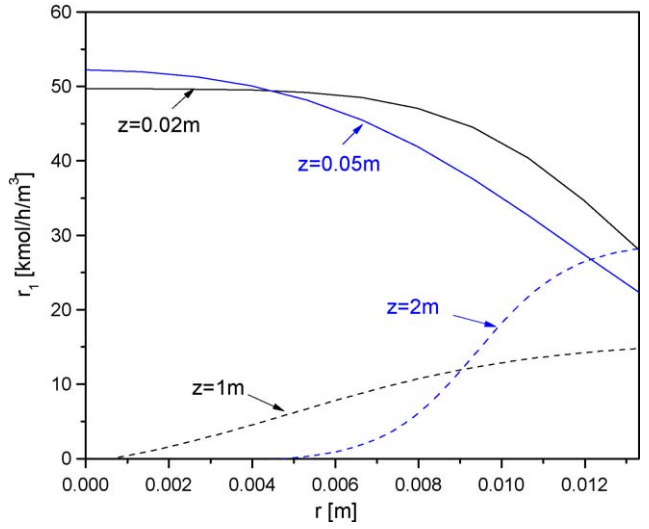

Fig. 9. Radial profiles of rate of reaction 1 (ethane ODH, see Eq. (1)), for different axial positions. T_0 = 370 °C; $T_{0,S}$ = 25 °C; $y_{0,O_2} = 0.01$; $\Delta P_{T\text{-}M}$ = 0.45 atm.

oxygen depletion in the central zone of the tube is observed. Consequently, the reaction rates are close to zero in the central zone of the tube and the heat generation rate is concentrated in a narrow zone close to the membrane (see Fig. 9: curves for the desired reaction). Under these conditions, the temperature decreases towards the tube center (r = 0 m) and a slight temperature maximum near the membrane wall (r = 0.0133 m) occurs (see Fig. 8: curves for $z > 1$ m). The radial dispersion of heat takes place from the location of the temperature maximum in two opposite directions: towards the membrane wall and the tube center. The "effective" zone of the catalyst bed (responsible for the heat generation) is an annulus near the membrane, while the central part of the tube acts as an "inert" zone. The heat transfer area per unit volume of "effective catalyst bed" is therefore higher than $4/d_T$, which is the characteristic value of a conventional fixed-bed reactor with cylindrical geometry. This, together with the high selectivity to ethylene, explains why the reaction temperature can be efficiently controlled even at axial positions where the driving force for the convective cooling ($T - T_S$) is small (see Fig. 6 for $z > 1$ m).

4. Conclusions

The multitubular membrane reactor leads to significant ethylene production per tube and milder temperature profiles than a conventional wall-cooled fixed-bed reactor. This is a consequence of the low partial pressures of oxygen along the membrane reactor, leading to improved selectivity to ethylene (lower heat generation rates) and high heat transfer area per unit of "effective" catalyst volume.

Under certain operating conditions, an undesirable oxygen accumulation phenomenon inside the catalyst bed may appear which can be minimized by carefully adjusting the operating conditions.

The presence of O_2 at the reactor inlet significantly improves the ethylene production rates. However, if higher amounts of O_2 are fed to the reactor mouth, the selectivity could drop, which may lead to hot spots near the entrance.

The use of a 2D model has enabled the proper quantification of the strong composition gradients occurring along the radial coordinate and their influence on the reactor performance.

Acknowledgments

Support for this work through Universidad Nacional del Sur (UNS) and Consejo Nacional de Investigaciones Científicas y Tecnológicas (CONICET) is gratefully acknowledged.

Appendix A. Supplementary data

Supplementary data associated with this article can be found, in the online version, at doi:10.1016/j.cattod.2010.01.053.

References

[1] G. Centi, F. Cavani, F. Trifiro, Selective Oxidation by Heterogeneous Catalysis, Kluwer Academic Publishers/Plenum Press, New York, USA, 2001.
[2] F. Cavani, N. Ballarini, A. Cericola, Oxidative dehydrogenation of ethane and propane: How far from commercial implementation? Catal. Today 127 (2007) 113.
[3] H. Zimmermann, R. Walzl, 6th rev. ed., "Ethylene" in Ullmann's Encyclopedia of Industrial Chemistry, vol. 12, Wiley–VCH, 2003,, p. 531.
[4] M.A. Bañares, Supported metal oxide and other catalysts for ethane conversion: a review, Catal. Today 51 (1999) 319.
[5] F. Cavani, F. Trifiro, Selective oxidation of light alkanes: interaction between the catalyst and the gas phase on different classes of catalytic materials, Catal. Today 51 (1999) 561.
[6] R. Grabowski, Kinetics of oxidative dehydrogenation of C_2–C_3 alkanes on oxide catalysts, Catal. Rev. 48 (2006) 199.

[7] M.D. Argyle, K. Chen, A.T. Bell, E. Iglesia, Effect of catalyst structure on oxidative dehydrogenation of ethane and propene on alumina-supported vanadia, J. Catal. 208 (2002) 139.
[8] E.M. Thorsteinson, T.P. Wilson, F.G. Young, P.H. Kasai, The oxidative dehydrogenation of ethane over catalysts containing mixed oxides of molybdenum and vanadium, J. Catal. 52 (1978) 116.
[9] Y. Liu, P. Cong, R.D. Doolen, S. Guan, V. Markov, L. Woo, S. Zeyb, U. Dingerdissen, Discovery from combinatorial heterogeneous catalysis. A new class of catalyst for ethane oxidative dehydrogenation at low temperatures, Appl. Catal. A 254 (2003) 59.
[10] E. Heracleous, A.F. Lee, I.A. Vasalos, A.A. Lemonidou, Surface properties and reactivity of Al_2O_3-supported MoO_3 catalysts in ethane oxidative dehydrogenation, Catal. Lett. 88 (2003) 47.
[11] M.V. Martínez-Huerta, X. Gao, H. Tian, I.E. Wachs, J.L.G. Fierro, M.A. Bañares, Oxidative dehydrogenation of ethane to ethylene over alumina-supported vanadium oxide catalysts: relationship between molecular structures and chemical reactivity, Catal. Today 118 (2006) 279.
[12] F. Klose, M. Joshi, C. Hamel, A. Seidel-Morgenstern, Selective oxidation of ethane over a VO_x/α-Al_2O_3 catalyst—investigation of the reaction network, Appl. Catal. A 260 (2004) 101.
[13] E. Heracleous, A.A. Lemonidou, Ni–Nb–O mixed oxides as highly active and selective catalysts for ethene production via ethane oxidative dehydrogenation. Part I. Characterization and catalytic performance, J. Catal. 237 (2006) 162.
[14] E. Heracleous, A.A. Lemonidou, Ni–Nb–O mixed oxides as highly active and selective catalysts for ethene production via ethane oxidative dehydrogenation. Part II. Mechanistic aspects and kinetic modelling, J. Catal. 237 (2006) 175.
[15] P. Arpentinier, F. Cavani, F. Trifiro, The Technology of Catalytic Oxidations, Technip, Paris, France, 2001.
[16] E. López, E. Heracleous, A.A. Lemonidou, D.O. Borio, Study of a multitubular fixed-bed reactor for ethylene production via ethane oxidative dehydrogenation, Chem. Eng. J. 145 (2008) 308–315.
[17] J. Coronas, M. Menéndez, J. Santamaría, Use of a ceramic membrane reactor for the oxidative dehydrogenation of ethane to ethylene and higher hydrocarbons, Ind. Eng. Chem. Res. 34 (1995) 4229.
[18] A.L.Y. Tonkovich, J.L. Zilka, D.M. Jimenez, G.L. Roberts, J.L. Cox, Experimental investigations of inorganic membrane reactors: a distributed feed approach for partial oxidation reactions, Chem. Eng. Sci. 51 (1996) 789.
[19] F. Klose, T. Wolff, S. Thomas, A. Seidel-Morgenstern, Operation modes of packed-bed membrane reactors in the catalytic oxidation of hydrocarbons, Appl. Catal. A 257 (2004) 193.
[20] A. Pantazidis, J.A. Dalmon, C. Mirodatos, Oxidative dehydrogenation of propane on catalytic membrane reactors, Catal. Today 25 (1995) 403.
[21] R. Ramos, M. Menéndez, J. Santamaría, Oxidative dehydrogenation of propane in an inert membrane reactor, Catal. Today 56 (2000) 239.
[22] C. Téllez, M. Menéndez, J. Santamaría, Oxidative dehydrogenation of butane using membrane reactors, AIChE J. 43 (1997) 777.
[23] S.H. Ge, C.H. Liu, L.J. Wang, Oxidative dehydrogenation of butane using inert membrane reactor with a non-uniform permeation pattern, Chem. Eng. J. 84 (2001) 497.
[24] R. Mallada, M. Menéndez, J. Santamaría, Use of membrane reactors for the oxidation of butane to maleic anhydride under high butane concentrations, Catal. Today 56 (2000) 191.
[25] J.G. Sanchez-Macano, T.T. Tsotsis, Catalytic Membranes and Membrane Reactors, Wiley–VCH, Weinheim, 2002.
[26] J. Coronas, J. Santamaría, Catalytic reactors based on porous ceramic membranes, Catal. Today 51 (3–4) (1999) 377.
[27] A. Julbe, D. Farrusseng, C. Guizard, Porous ceramic membranes for catalytic reactors—overview and new ideas, J. Membr. Sci. 181 (2001) 3.
[28] A.G. Dixon, Recent research in catalytic inorganic membrane reactors, Int. J. Chem. React. Eng. 1 (2003) 1 (Review R6).
[29] G. Saracco, H.W.J.P. Neomagnus, G.F. Versteeg, W.P.M. van Swaaij, High-temperature membrane reactors: potential and problems, Chem. Eng. Sci. 54 (1999) 1997.
[30] K.K. Sirkar, P.V. Shanbhag, A.S. Kovvali, Membrane in a reactor: a functional perspective, Ind. Eng. Chem. Res. 38 (1999) 3715.
[31] C. Téllez, M. Menéndez, J. Santamaría, Simulation of an inert membrane reactor for the oxidative dehydrogenation of butane, Chem. Eng. Sci. 54 (1999) 2917.
[32] J. Coronas, M. Menéndez, J. Santamaría, The porous-wall ceramic membrane reactor: an inherently safer contacting device for gas-phase oxidation of hydrocarbons, J. Loss Prev. Process. Ind. 8 (1995) 97.
[33] A. Julbe, D. Farrusseng, D. Cot, C. Guizard, The chemical valve membrane: a new concept for an auto-regulation of O_2 distribution in membrane reactors, Catal. Today 67 (2001) 139.
[34] Y. Lu, A.G. Dixon, W.R. Moser, Y.H. Ma, Analysis and optimization of cross-flow reactors with distributed reactant feed and product removal, Catal. Today 35 (1997) 443.
[35] C. Hamel, S. Thomas, K. Schädlich, A. Seidel-Morgenstern, Theoretical analysis of reactant dosing concepts to perform parallel-series reactions, Chem. Eng. Sci. 58 (2003) 4483.
[36] K. Hou, R. Hughes, R. Ramos, M. Menéndez, J. Santamaría, Simulation of a membrane reactor for oxidative dehydrogenation of propane, incorporating radial concentration and temperature profiles, Chem. Eng. Sci. 56 (2001) 57.
[37] M. Pedernera, M.J. Alfonso, M. Menéndez, J. Santamaría, Simulation of a catalytic membrane reactor for the oxidative dehydrogenation of butane, Chem. Eng. Sci. 57 (2002) 2531.
[38] M.L. Rodriguez, D.E. Ardissone, A.A. Lemonidou, E. Heracleous, E. López, M.N. Pedernera, D.O. Borio, Simulation of a membrane reactor for the catalytic oxide-hydrogenation of ethane, Ind. Eng. Chem. Res. 48 (2009) 1090.
[39] G.F. Froment, K.B. Bischoff, Chemical Reactor Analysis and Design, Wiley, Toronto, Canada, 1990.
[40] A. Marsella, P. Fatutto, D. Carmello, Catalyst and oxychlorination process using it, United States Patent 6465701, USA (2002).
[41] S. Yagi, D. Kunii, Studies on heat transfer near wall surface in packed beds, AIChE J. 6 (1960) 543.
[42] R.W. Serth, Process Heat Transfer. Principles and Applications, Elsevier Science, 2007.
[43] D.O. Borio, J.E. Gatica, J.A. Porras, Wall-cooled fixed-bed reactors: parametric sensitivity as a design criterion, AIChE J. 35 (1989) 287.
[44] P. Zehner, E.U. Schlünder, Wärmeleitfähigkeit von schüttungen bei mässigen temperature, Chem. Ing. Technol. 42 (1970) 933.
[45] M. Pedernera, R. Mallada, M. Menendez, J. Santamaría, Simulation of an inert membrane reactor for the synthesis of maleic anhydride, AIChE J. 46 (2000) 2489.
[46] R.G. Munro, Evaluated material properties for a sintered α-alumina, J. Am. Ceram. Soc. 80 (1997) 1919.
[47] R.V. Mallada, PhD thesis, University of Zaragoza, Spain (1999).